Mechanism of intrinsic resistance of lung squamous cell carcinoma to epithelial growth factor receptor-tyrosine kinase inhibitors revealed by high-throughput RNA interference screening

LIXIA JU[1*], ZHIYI DONG[1*], JUAN YANG[2*] and MINGHUA LI[3*]

Departments of [1]Integrative Medicine and [2]Emergency, Shanghai Pulmonary Hospital, Tongji University Medical School Cancer Institute, Tongji University, Shanghai 200433; [3]Department of Oncology, Shanghai Municipal Hospital of Traditional Chinese Medicine, Shang University of Traditional Chinese Medicine, Shanghai 200071, P.R. China

Received April 12, 2020; Accepted August 24, 2020

DOI: 10.3892/ol.2020.12218

Abstract. Although targeted therapy has achieved a great breakthrough in the treatment of lung adenocarcinoma, there are still no effective targeted drugs for lung squamous cell carcinoma (SqCC). In addition, as immunotherapy can only prolong the overall survival (OS) of lung SqCC by ≤5 months, chemotherapy and radiotherapy are still the main types of therapy for advanced SqCC. The expression level of epithelial growth factor receptor (EGFR) in patients with lung SqCC is higher compared with those with adenocarcinoma, but the former group is intrinsically resistant to EGFR-tyrosine kinase inhibitors (EGFR-TKIs). Therefore, if the drug resistance in patients with lung SqCC could be reversed, the majority of patients may benefit from EGFR-TKIs. In the present study, the high-throughput RNA interference technology was used to screen the genes involved in the EGFR-TKI erlotinib resistance of lung SqCCs, and integrin-linked kinase (ILK) was identified to be the most effective. The role of ILK in erlotinib resistance was further studied in cell lines, and the expression of ILK was analyzed in patients with SqCC and adenocarcinoma. Finally, the mechanism of ILK in EGFR-TKIs resistance was analyzed using Kyoto Encyclopedia of Genes and Genomes (KEGG), Gene Ontology (GO) and ingenuity pathway analysis (IPA). The results demonstrated that the ILK gene knockdown could overcome erlotinib resistance by inhibiting cell proliferation, inducing apoptosis and blocking the cell cycle at the G2/M phase. The expression of ILK in patients with SqCC was significantly higher compared with those with adenocarcinoma with sensitizing EGFR mutations. In addition, the cell cycle pathway 'G2/M DNA damage and checkpoint regulation' was identified to be significantly inhibited by ILK knockdown in IPA, KEGG and GO analysis. The results of the present study may improve the understanding of EGFR-TKI resistance in lung SqCCs, thus promoting the development of potential targeted therapies for lung SqCCs.

Correspondence to: Professor Lixia Ju, Department of Integrative Medicine, Shanghai Pulmonary Hospital, Tongji University Medical School Cancer Institute, Tongji University, 507 Zhengmin Road, Yangpu, Shanghai 200433, P.R. China
E-mail: jvlixia@126.com

*Contributed equally

Key words: integrin-linked kinase, epithelial growth factor receptor-tyrosine kinase inhibitors, lung squamous cell carcinoma

Introduction

Lung squamous cell carcinoma (SqCC) accounts for ~30% of non-small cell lung cancer (NSCLC) (1). In recent years, the treatment of lung SqCC has been less successful compared with lung adenocarcinoma (2). Although complex biological studies have improved our understanding of the pathological mechanisms of SqCC, for example identifying PI3K catalytic subunit α (PIK3CA), hepatocyte growth factor receptor and fibroblast growth factor receptor as important driver mutations, there are currently no effective agents for its treatment (3). In the era of immunotherapy, pembrolizumab has been listed as the first-line treatment for patients with NSCLC with programmed death-ligand 1 tumor proportion score (TPS) ≥50%, according to the 2019 National Comprehensive Cancer Network (NCCN) guidelines (4). However, the median overall survival (OS) time of the patients with NSCLC treated with pembrolizumab alone is only 20 months (5), which is poor compared with targeted therapy in adenocarcinomas (6). In the most notable clinical trial of SqCC, CheckMate-017, the median OS time of patients treated with nivolumab as the second-line treatment for advanced lung SqCC was prolonged by only 3 months compared with those treated with docetaxel (7). In the KEYNOTE-010 clinical trial, the OS time in the 2 and 10 mg/kg pembrolizumab groups was prolonged by 2 and 4 months, respectively, compared with that in patients treated with docetaxel (8). At present, chemotherapy and radiotherapy remain the main treatment options for advanced lung SqCC.

Since epithelial growth factor receptor-tyrosine kinase inhibitors (EGFR-TKIs) inhibit the phosphorylation of EGFR

tyrosine kinase, they are supposed to exhibit high efficacy in the tumors with high expression levels of EGFR (9). However, this is not the case in lung SqCC. Previous studies have demonstrated that ≤84% of patients with lung SqCC express EGFR, which is significantly higher than the percentage of patients with EGFR-positive adenocarcinoma (~44%) (10,11); however, only patients with adenocarcinoma with sensitizing EGFR mutations respond to EGFR-TKI treatment, whereas for the other patients with adenocarcinomas and SqCCs, the efficacy of EGFR-TKIs is not satisfactory (9). In addition, EGFR mutations, in terms of their predictive value for the response to EGFR-TKI treatment, are different between SqCC and adenocarcinoma. For example, EGFR mutations are not valid predictors for EGFR-TKI response in lung SqCC, with the response rate <30% in patients with lung SqCC with sensitizing EGFR mutations, as well as the median progression-free survival time of only 2-3 months (12-14), which is shorter compared with that in patients with adenocarcinoma with sensitizing EGFR mutations (10-12 months) (9). Therefore, the intrinsic resistance to EGFR-TKIs in patients with lung SqCC has become an urgent problem. The present study was based on the hypothesis that certain genes may be associated with intrinsic EGFR-TKIs resistance.

In the past decade, the application of next generation sequencing to investigate the genomic characterization of lung SqCC has provided a further understanding of the possible treatment targets. Filipits (15) have reported that the potential targeted therapies in lung SqCC include EGFR, fibroblast growth factor receptor 1, Met proto-oncogene, PI3K, discoidin domain receptor tyrosine kinase 2, BRAF, AKT, cytotoxic T lymphocyte-associated protein and programmed cell death 1. Additionally, Schwaederle *et al* (16) have identified some mutations in TP53 (64.5% of analyzed patients) that are not targeted by any existing agents, PIK3CA (28.5%), cyclin-dependent kinase inhibitor 2A (24.4%), SOX2 (17.7%) and cyclin D1 (15.8%). EGFR is highly expressed in the majority of SqCC tumor tissues, but the clinical benefits of EGFR-TKIs are modest (17,18). At present, no effective targeted agents for SqCC have been approved for use in clinical practice. Therefore, it is crucial to explore the possible mechanisms of intrinsic EGFR-TKI resistance in lung SqCC.

The high-throughput RNA interference (RNAi) technology is the combination of high-throughput chromatin immunoprecipitation and small interference RNA library that makes RNAi no longer limited to one gene being silenced, but can be used for simultaneous large-scale screening of genes and their functions. In the present study, the most effective gene inhibitors that can overcome EGFR-TKI resistance of lung SqCC were screened using high-throughput RNAi technology. The results may bring aid the development of novel treatments for patients with SqCC.

Materials and methods

Cell lines and culture. The human lung squamous carcinoma cell lines SK-MES-1, H1688, H1299 and H226 were provided by Cancer Institute of Tongji University Medical School, (Shanghai, China). The cells were cultured at 37˚C with 5% CO_2 in Dulbecco's modified Eagle's medium (DMEM) supplemented with 10% fetal bovine serum (FBS) (Gibco; Thermo Fisher Scientific, Inc.), 100 U/ml penicillin and 100 mg/ml streptomycin.

Tumor samples. Tumor samples were collected from 50 patients recruited at the Shanghai Pulmonary Hospital between July 2012 and June 2015. The patients were newly diagnosed with histologically confirmed lung SqCC and adenocarcinoma by biopsy. The mean age was 63.77 (49-74) years, 63.44 (47-71) years and 62.9 (49-72) years in SqCC, wide-type EGFR adenocarcinoma and mutated-EGFR adenocarcinoma groups, respectively. There was no females in the SqCC group, but three (33.3%) females in the wide-type EGFR adenocarcinoma group, and seven (70%) female in the mutated-EGFR adenocarcinoma group. The rest of the patients were male. Patients with a previous medical history of cancer, radiotherapy or chemotherapy were excluded. This study was approved by the Ethics Committee of Tongji University (approval no. 2012-FK-14), and all patients provided signed informed consent.

High content screening (HCS). In total, 18 target shRNAs (Table I) were selected using the following criteria according to Genechem database based on the NIH Cancer Genome Project database, OMIM, MalaCards and UniProtKB database (https://www.genechem.com.cn/index/index/index.html). Firstly, the genes were highly correlated with EGFR-TKIs and certified by pathway and functional network analysis from Genechem, and the gene function annotations should be relatively clear. Subsequently, the genes that were reported in PubMed <100 times, or those whose function were obviously inconsistent with their expected function, were removed. Lentiviruses carrying the green fluorescent protein (GFP) gene and expressing short hairpin (sh)RNA against ILK, phosphatase and tensin homolog (PTEN), mitogen-activated protein kinase kinase kinase 14 (MAP3K14), myeloid differentiation primary response gene 88 (MYD88), serum response factor (SRF), interleukin-1 receptor associated kinase 1 (IRAK1), baculoviral IAP repeat containing 5 (BIRC5), phosphoinositide-3-kinase, class 2, α polypeptide (PIK3C2A), protein tyrosine phosphatase type IVA, member 3 (PTP4A3), Bruton's tyrosine kinase (BTK), nemo-like kinase (NLK), Raf-1 proto-oncogene (RAF1), signal transducer and activator of transcription 3 (STAT3), sarcoma gene (SRC), aurora kinase A (AURKA), interleukin-1 receptor-associated kinase 4 (IRAK4), erbb2-interacting protein (ERBB2IP) or Cadherin (CDH), as well as negative control (NC) shRNA, were purchased from Shanghai GeneChem Co., Ltd. SK-MES-1 cells were transfected with shRNA lentiviruses (non-targeting shRNA, PSC1369, PSC1446, PSC14867 mix, PSC14872, PSC3584, PSC1489 6 mix, PSC14359, PSC14907, PSC1675, PSC14821 mix, PSC1786, PSC1809, PSC8012, PSC4913, PSC2260, PSC14817 mix, PSC4899, and PSC3306 that target the NC, ILK, PTEN, MAP3K14, MYD88, SRF, IRAK1, BIRC5, PIK3C2A, PTP4A3, BTK, NLK, RAF1, STAT3, SRC, AURKA, IRAK4, ERBB2IP, and CDH genes, respectively; Table I) using Polybrene (Shanghai GeneChem Co., Ltd.) at 37˚C for 12 h, and MOI was 10. Following 2 or 3 days of transfection, when the fluorescence rate reached 80%, the cells were collected for subsequent cell proliferation experiments. In the HCS experiment, 2 μM erlotinib was used to screen the combined effects of erlotinib and shRNAs after

Table I. Target and lentiviral shRNA and fold-changes of cell proliferation after 72-h treatment with shRNA and erlotinib.

Target	Identifier of shRNA	Fold-change
NC	Non-targeting shRNA	1.00
ILK	PSC1369	1.29[a]
PTEN	PSC1446	1.14
MAP3K14	PSC14867mix	1.09
MYD88	PSC14872	1.05
SRF	PSC3584	1.04
IRAK1	PSC14896mix	1.03
BIRC5	PSC14359	1.03
PIK3C2A	PSC14907	1.00
PTP4A3	PSC1675	1.00
BTK	PSC14821mix	0.97
NLK	PSC1786	0.97
RAF1	PSC1809	0.93
STAT3	PSC8012	0.92
SRC	PSC4913	0.92
AURKA	PSC2260	0.89
IRAK4	PSC14817mix	0.87
ERBB2IP	PSC4899	0.86
CDH	PSC3306	0.83

[a]P<0.05. shRNA, short hairpin RNA; NC, negative control.

72 h treatment. The high-throughput RNAi experiments were performed by Shanghai GeneChem Co., Ltd.

Celigo, a high-throughput screening system based on automatic image acquisition and image data analysis, was used for the HCS test. The target in this test was the SK-MES-1 cells (growing in a 96-well plate) expressing GFP following lentiviral infection. Celigo was used to identify the cells with green fluorescence, capture, analyze and process images and calculate the number of cells in the various groups in the plate. After 5 days of continuous reading, the cell growth curves were produced to determine the cell proliferation.

Cell proliferation analysis. The cells were seeded into 96-well plates ($3x10^3$ cells/well) in triplicate and exposed to various concentrations (2, 4 and 10 μmol) of erlotinib. After 72 h, 20 μl 3-(4,5-dimethylthiazol-2-yl)-2,5-diphenyltetrazolium bromide (MTT) solution (Abcam) (5 mg/ml) was added to each well and incubated for 4 h at 37˚C. Subsequently, the formazan crystal was dissolved with dimethyl sulfoxide, and the absorbance at 530 nm was read using a microplate reader. The percentage of surviving cells was calculated as follows: Survival rate=(mean absorbance of the replicate wells containing drugs-mean absorbance of the replicate background wells)/(mean absorbance of the replicate drug-free wells-mean absorbance of the replicate background wells) x100%. Fold-change=[(NC + drug)/NC)/(target shRNA + drug)/target shRNA]. The test was performed independently three times.

Apoptosis analysis. Annexin V-APC Apoptosis Detection kit (eBioscience; Thermo Fisher Scientific, Inc.) and a transferase-mediated deoxyuridine triphosphate nick-end labeling (TUNEL) kit (Promega Corporation) were used to determine apoptosis levels. In the flow cytometry assay, SK-MES-1 cells ($1.2x10^6$ cells/well) were plated in 6-well plates. Following 24 h incubation at 37˚C, 2 μM erlotinib was added into the experimental wells and incubated for another 72 h at 37˚C. The cells were harvested, washed with PBS and resuspended in 500 μl binding buffer (from the aforementioned kit). The cells were stained with 5 μl Annexin V-PE and incubated for 5 min at room temperature in the dark. Quantification of apoptosis was determined by flow cytometer (FACSCalibur; BD Bioscience). Fluorescence microscope (micropublisher 3.3RTV, Olympus Corporation) was used to count the cells with Annexin V-APC. BD CellQuest software was used for analysis.

For the TUNEL assay, SK-MES-1 cells ($5x10^5$ cells/well) were seeded in 24-well plates and exposed to 2 μM erlotinib for 72 h. Apoptosis was assessed by the TUNEL assay kit according to the manufacturer's protocol. The apoptotic index (%) was calculated using the following formula: Apoptotic index=positive for Annexin V- or PE-stained cells/total cells x100%. The apoptotic index for Annexin V and PE-stained cells were calculated separately.

Western blotting. Cells were washed twice with ice-cold PBS and lysed in 0.1 ml lysis buffer (HyClone; Cyvita) on ice for 30 min. Insoluble debris was removed by centrifuging at 12,000 x g for 15 min at 4˚C. BCA Protein Assay kit (HyClone; Cyvita) was used for protein detection, and 20 μg protein was loaded per lane. The percentage of the SDS-PAGE gel was 10% and then the proteins were transferred to PVDF membrane. PVDF membrane was sealed with blocking solution (TBST solution containing 5% skimmed milk) at room temperature for 1 h or 4˚C overnight. Mouse Anti-Flag (1:3,000; cat. no. F1804; Sigma-Aldrich; Merck KGaA) was diluted with blocking solution, and then incubated with the closed PVDF membrane at room temperature for 2 h or 4˚C overnight. Mouse anti-GAPDH (1:5,000; cat. no. sc-32233; Santa Cruz Biotechnology, Inc.) was for the reference. Goat anti-mouse IgG (1:5,000; cat. no. sc-2005; Santa Cruz Biotechnology, Inc.) was diluted with blocking solution, and then incubated with the closed PVDF membrane at room temperature for 2 h. Antibodies against human ILK (1:3,000; cat. no. MAB4266-SP), EGFR (1:1,000; cat. no. MAB3570-SP), β-actin (1:1,000; cat. no. MAB8929-SP) and GAPDH (1:1,000; cat. no. AF5718-SP) (all from R&D Systems, Inc.) were used according to the manufacturer's instructions. The ECL + Plus™ Substrate (Amersham) was used for color development. Densitometry analysis was performed using an Odyssey® Infrared Imaging system (LI-COR Biosciences).

Quantitative (q)PCR. Total RNA was extracted from tumors using TRIzol (Shanghai Perfectics Co., Ltd), and reverse transcribed to cDNA using M-MLV Reverse Transcriptase kit (Promega Corporation). Reverse transcription was carried out at 37˚C for 10 min. In total, 1 μg cDNA was used for qPCR analysis using a LightCycler PCR instrument (Roche Diagnostics) according to the manufacturer's instructions. The upstream primer of ILK and GAPDH was 5'-GACGACATT TTCACTCAGTGCC-3' and 5'-TGACTTCAACAGCGACAC

CCA-3' respectively, and the downstream primer was 5'-ACG GTTCATTACATTGATCCGTG-3' and 5'-CACCCTGTTGCT GTAGCCAAA-3', respectively. Amplifications were carried out in 20-μl reaction mixtures under the following conditions: Initial denaturation at 95˚C for 2 min; followed by 40 cycles of 95˚C for 20 sec, 55˚C for 20 sec and 72˚C for 35 sec; and a final extension at 72˚C for 3 min. GAPDH was used as the internal control. SYBR Master Mixture (DRR041B, Takara) was used for your gene expression analysis. The copy numbers of the ILK gene were determined as follows: Target gene copy number $2^{-\Delta\Delta Cq}$=($Cq_{target\ gene}$-$Cq_{reference\ gene}$) experimental group-($Cq_{target\ gene}$-$Cq_{reference\ gene}$) control group (19).

Cell cycle analysis. SK-MES-1 cells ($1.2x10^6$ cells/well) were incubated in 6-well plates at 37˚C for 24 h, and the cell culture medium was replaced with fresh medium containing 10% FBS with or without erlotinib at 37˚C for another 72 h. The cells were trypsinized, fixed in ice-cold 70% ethanol overnight and stained with propidium iodide containing 1 mg/ml RNase (Sigma-Aldrich; Merck KGaA) according to the instructions of the Cell Cycle Phase Determination kit (Cayman Chemical Company). The samples were analyzed using a flow cytometer (FACSCalibur; BD Bioscience). The cell cycle parameters from 10,000 events were analyzed using multi-cycle software (version 3.1.1, Phoenix Flow Systems).

Clone formation analysis. Cells (200 cells/well) were seeded in 24-well plates and treated with erlotinib at 37˚C after 12 h. After 2 weeks of culture, the cells were stained with GIEMSA at room temperature for 20 min, and the number of visible colonies were counted manually. The relative clone formation ability was calculated by clone number/well.

Signaling pathway microarray analysis. The lung SqCC cells were separated into two groups: i) NC (SK-MES-1 cells treated with erlotinib); and ii) knockdown (KD; SK-MES-1 cells treated with erlotinib after ILK knockdown by shRNA). Total RNA was extracted from cells by TRIzol (Shanghai Perfectics Co., Ltd), and RNA probes were prepared and hybridized to the GeneChip primeview human 100 format (cat. no. 901838; Affymetrix GeneChip System; Affymetrix; Thermo Fisher Scientific, Inc.) according to the manufacturer's instructions. For each sample, three biological replicates were performed. All arrays were washed, stained, and read by a GeneChip Scanner 3000 (Affymetrix; Thermo Fisher Scientific, Inc.). The fluorescence signal was excited at 532 nm and detected at 570 nm. Data were analyzed using GeneChip Operating Software 1.4 (Affymetrix; Thermo Fisher Scientific, Inc.)

Bioinformatics analysis. To analyze differentially expressed genes (DEGs) between NC and KD groups, the GEO2R tool (http://www.ncbi.nlm.nih.gov/geo/geo2r/) were used. To control errors, the false discovery rate (FDR) determination feature automatically included in the GEO2R tool was employed. Significant DEGs were those that remained significant after FDR correction. DEGs were selected based on |fold-change|>2 and P<0.05 for GeneChip analysis (GeneChip Hybridization Wash and Stain kit; Thermo Fisher Scientific, Inc.). Based on the Kyoto Encyclopedia of Genes and Genomes (KEGG) database (https://www.kegg.jp/kegg/pathway.html), significantly changed pathways were identified and connected in a pathway network (Path-net) to show the association between these pathways. GO analysis (http://geneontology.org/) was used to organize DEGs into hierarchical categories. The list of DEGs, containing gene identifiers and corresponding expression values, was also uploaded into the IPA software 2012 (Ingenuity Systems, Inc.). The 'core analysis' function included in the software was used to interpret the differentially expressed genes between NC and KD groups, which included biological processes, canonical pathways, upstream transcriptional regulators and gene networks. Each gene identifier was mapped to its corresponding gene target in the Ingenuity Pathway Knowledge Base (www.ingenuity.com).

Statistical analysis. Data are presented as the mean ± SEM. Statistical analysis was performed using SPSS Statistics 23 software (IBM Corp.). Data were analyzed using unpaired Student's t-test or one-way ANOVA with Tukey's post hoc test, and P<0.05 was considered to indicate a statistically significant difference.

Results

ILK knockdown improves the effects of erlotinib in lung SqCC. The MTT assay results demonstrated that the IC_{50} of SK-MES-1 cells was 11.35 μM, the results of western blotting revealed that this cell line expressed EGFR (Fig. 1A and B). The SK-MES-1 cells were treated with a gradient of different concentrations of erlotinib following transfection with lentiviral NC shRNA. Cell proliferation was inhibited by 2 μM erlotinib; thus, 2 μM was used as the screening concentration in subsequent experiments (Fig. 1C).

In HCS, the fold-changes of cell proliferation were detected by MTT after 72-h treatment with shRNAs and erlotinib. Transfection with the shRNAs targeting ILK, PTEN, MAP3K14 and MYD88, increased the effects of erlotinib on SK-MES-1 cells compared with NC. Following ILK knockdown, the cell proliferation was significantly inhibited by treatment with erlotinib compared with NC (fold-change, 1.29; P<0.05; Fig. 1D and Table I).

To identify the role of ILK in EGFR-TKI resistance, the cell survival rates of SK-MES-1 cells transfected with NC and ILK, MYD88 target shRNAs were measured following 72-h incubation with 2, 4 or 10 μM erlotinib. The results demonstrated that ILK shRNA significantly reduced the survival rate of SK-MES-1 cells, indicating that ILK knockdown improved the effects of erlotinib (Fig. 2A). The results of qPCR confirmed that ILK was expressed in lung cancer cell lines, including the SqCC cell lines SK-MES-1 and H226 (Fig. 2B).

Effects of ILK on erlotinib resistance in lung SqCC SK-MES-1 cells. The results of qPCR and western blotting confirmed that the expression of ILK was significantly inhibited in SK-MES-1 cells after RNA interference (P<0.01; Fig. 3A and B). Treatment with erlotinib following ILK knockdown significantly inhibited the proliferation of SK-MES-1 cells (P<0.05; Fig. 3C), induced apoptosis (P<0.01; Fig. 3D) and cell cycle arrest at the G2/M and G1 phases (P<0.01; Fig. 4A) compared with those in the group treated with erlotinib alone. The flow cytometry apoptosis assay results were verified by TUNEL assay; the observed

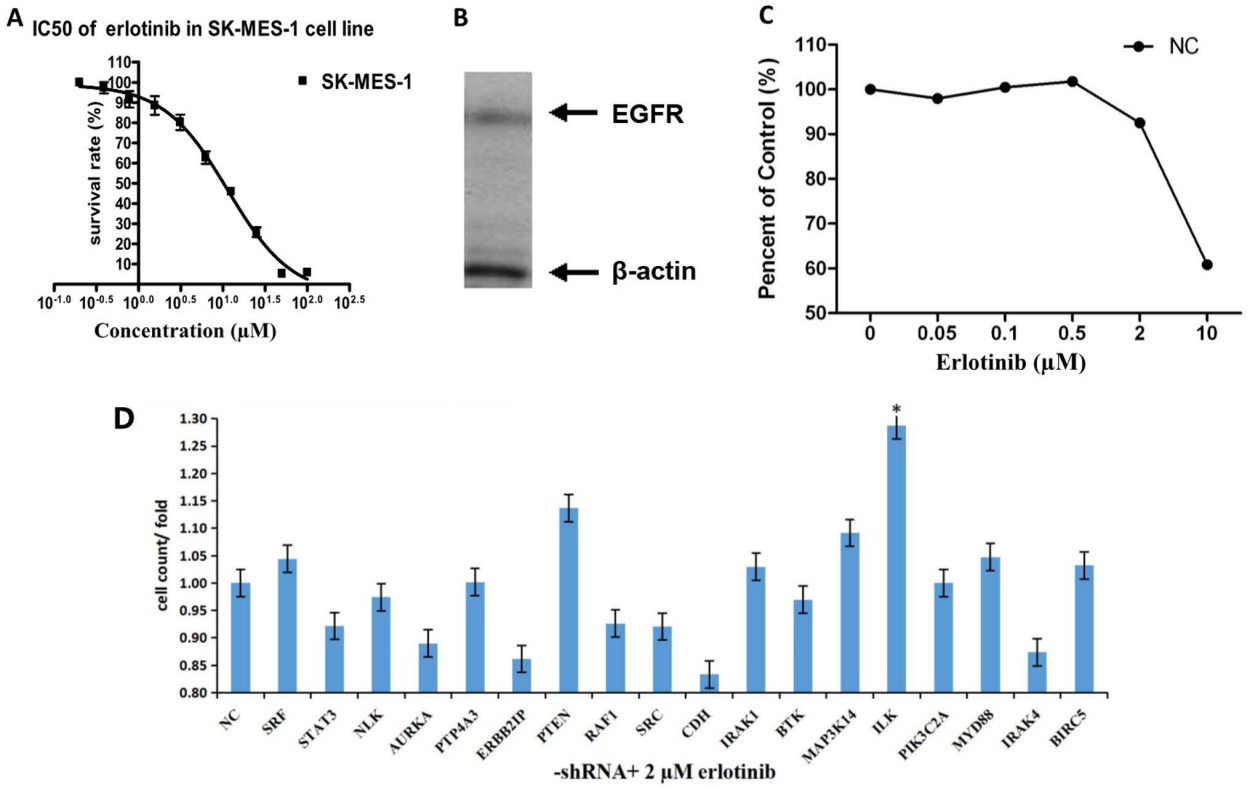

Figure 1. High-throughput RNA interference analysis of the effects of erlotinib in lung squamous cell carcinoma following integrin-linked kinase knockout. (A) The MTT assay results demonstrated that the IC_{50} of erlotinib in the SK-MES-1 cell line was 11.35 μM. (B) Western blotting results revealed that SK-MES-1 cells expressed EGFR. (C) SK-MES-1 cells were treated with a gradient of concentrations of erlotinib after transfection with lentiviral NC shRNA. The proliferation of cells significantly decreased after administration of 2 μM erlotinib. (D) In the high content screening experiment, the critical drug concentration of 2 μM was used to screen the combined effects of erlotinib and shRNAs after 72-h treatment. *P<0.05. NC, non-targeting control; shRNA, short hairpin RNA.

apoptotic rate was 83.24% in cells treated with erlotinib after ILK knockdown, which was notably higher compared with that of cells treated with erlotinib alone (P<0.01; Fig. 4B). The results also demonstrated that the cell clone formation ability decreased significantly in the group treated with erlotinib after ILK knockdown compared with that in the group treated with erlotinib alone (P<0.01; Fig. 4C).

Expression of ILK in patients with lung SqCC. ILK expression was detected in tumors of patients with lung squamous cell carcinoma, adenocarcinoma with wild-type EGFR or with sensitizing EGFR mutations using qPCR. A total of 31 cases of SqCC, 9 cases of wild-type EGFR adenocarcinoma and 10 cases of adenocarcinoma with sensitizing EGFR mutations were included in the analysis. The results demonstrated that the expression levels of ILK in patients with adenocarcinoma with sensitizing EGFR mutations were significantly lower compared with those in patients with adenocarcinoma with wild-type EGFR or SqCC (P<0.01; Fig. 5A). No significant differences were observed in ILK expression levels between patients with adenocarcinoma with wild-type EGFR and SqCC.

Genome-wide transcriptional analysis of the key pathways of ILK in EGFR-TKI resistance of the SK-MES-1 cell line. In order to further explore the mechanism of ILK in intrinsic EGFR-TKI resistance of lung SqCC, genome-wide transcriptional microarray analysis was carried out to compare the global gene expression between the control (NC group) and ILK-knockdown (KD group) SK-MES-1 cells following treatment with erlotinib using the Affymetrix GeneChip PrimeView Human Gene Expression Array. A total of 484 transcripts (317 upregulated and 167 downregulated) that were differentially expressed in the KD group compared with the NC group were selected for the cluster analysis (Fig. 5B).

The pathway enrichment analysis of the gene expression profiling based on KEGG and the BioCarta Database revealed that the top three targets enriched by ILK knockdown were the 'cell cycle', 'ECM receptor interaction' and 'oocyte meiosis', as shown in Fig. 5C.

The DEGs were also subjected to GO analysis. Among the molecular function-associated terms, the DEGs affected 'protein kinase activity' and 'DNA binding', which associated with the action mechanism of EGFR-TKIs (20,21). In the cellular component analysis, changes occurred in the 'intracellular non-membrane bound organelle', 'spindle' and 'cytoplasm'. These parts are closely associated with cell proliferation and intracellular signal transduction, which are the important factors for EGFR-TKI efficacy (22,23). In the biological process analysis, the changes involved 'mitotic cell cycle', 'mitosis', 'response to stress' and 'cell proliferation', suggesting that ILK knockdown may affect EGFR-TKI resistance via these cell processes.

The results of the IPA analysis revealed highly significant overlap of 207 canonical pathways associated with the DEGs in the SK-MES-1 cell line, including the 'mitotic roles of polo-like kinase', 'protein ubiquitination pathway', 'inhibition of matrix

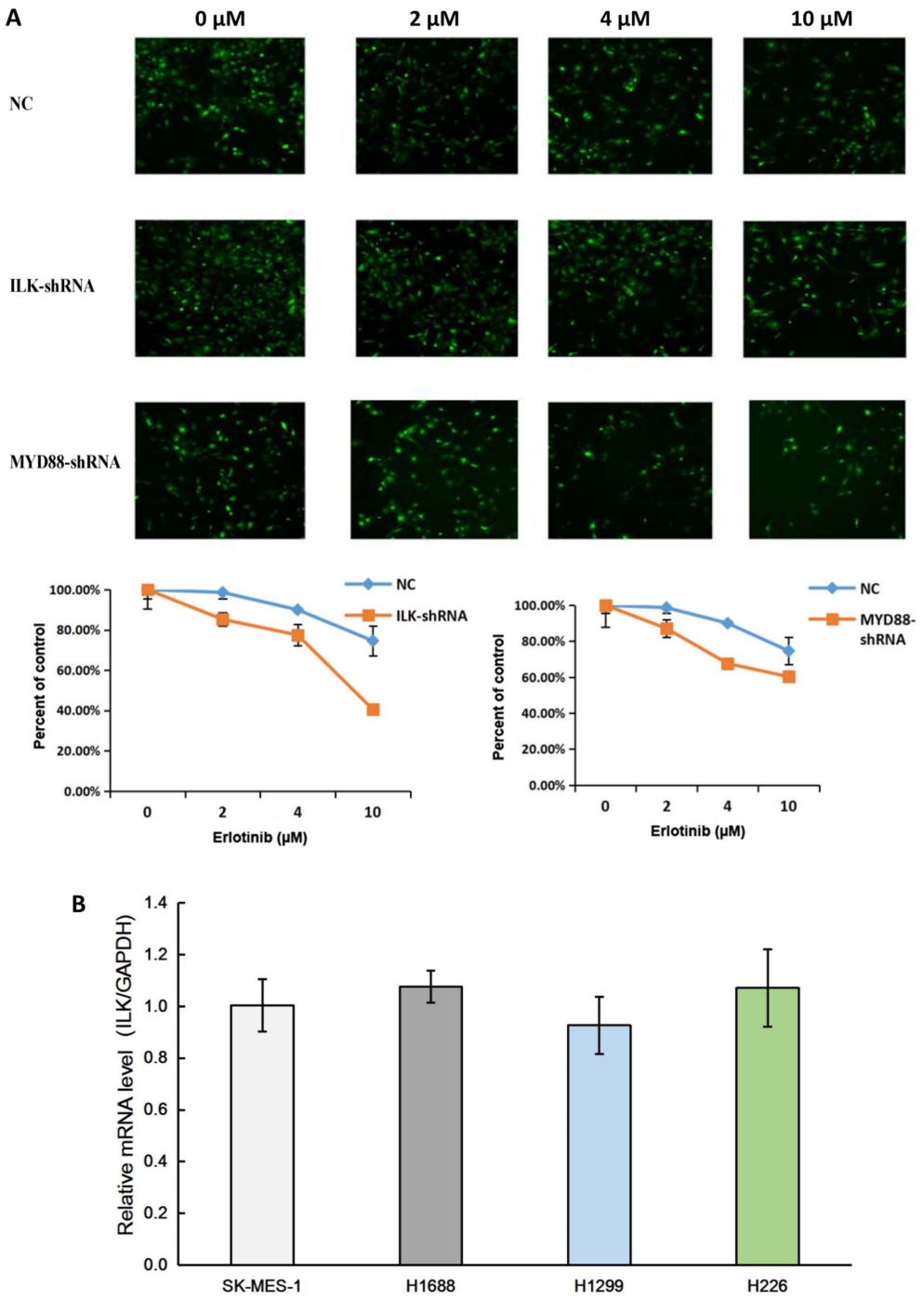

Figure 2. ILK knockout improves the effects of erlotinib in lung SqCC. (A) ILK knockout decreased the cell survival rate of SK-MES-1 cells. (B) Quantitative PCR confirmed that ILK was expressed in lung cancer cell lines, including the SqCC cell lines SK-MES-1 and H226. ILK, integrin-linked kinase; SqCC, squamous cell carcinoma; shRNA, short hairpin RNA; NC, non-targeting control.

metalloproteases' and 'cell cycle: G2/M DNA damage checkpoint regulation'. These pathways were scored based on the number of genes participating in any particular network. The results demonstrated that the 'cell cycle pathway: G2/M DNA damage checkpoint regulation' (Z-score, -2), was significantly inhibited in the Classic Pathway Analysis (Fig. 6A). The IPA-based network analysis demonstrated the interaction between molecules in the data set; all networks were sorted according to score values. The network diagram ranked first in this study was mainly associated with the 'cell cycle', 'cellular assembly organization', 'DNA replication', 'recombination' and 'repair' (Fig. 6B).

Discussion

Despite recent advances in immunotherapy, the prognosis of the majority of patients with SqCC is considerably worse compared with those with adenocarcinoma due to targeted therapy (24). However, patients with SqCC express higher levels EGFR compared with those with adenocarcinoma (9); thus, it is important to identify the mechanism of intrinsic resistance to EGFR-TKIs. In the present study, high-throughput RNAi screening revealed that the knockout of ILK improved the efficacy of erlotinib in the SqCC cell line SK-MES-1. Based

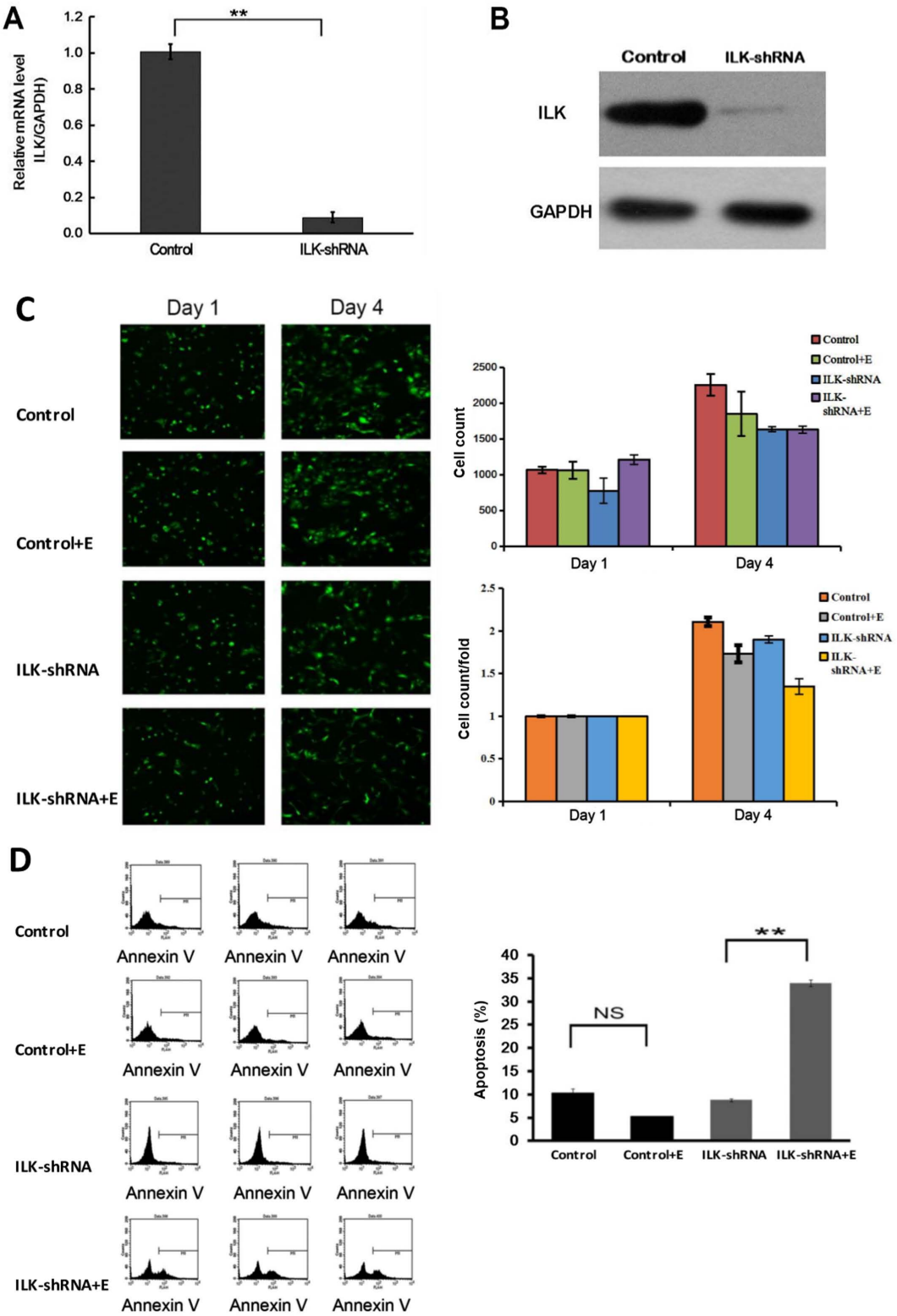

Figure 3. Expression and effects of ILK on erlotinib resistance in lung squamous cell carcinoma cells. (A and B) The results of quantitative PCR and western blotting confirmed that the expression of ILK was significantly inhibited in SK-MES-1 cells after RNA interference ($P<0.05$). (C) Treatment with erlotinib after ILK knockdown inhibited the proliferation of SK-MES-1 cells. (D) Erlotinib increased the apoptotic rate in SK-MES-1 cells transfected with ILK siRNA. $^{**}P<0.01$. ILK, integrin-linked kinase; siRNA, small interfering RNA; NC, negative control; E, erlotinib.

on these observations, the effects of ILK knockout on the biological activities of SK-MES-1 cells was investigated. The results demonstrated that cell proliferation and clone formation was inhibited, apoptosis was upregulated, and the cells were arrested at the G1 and G2/M phases following transfection with ILK siRNA compared with. These results confirmed that inhibition of ILK may be involved in reversing the resistance to erlotinib.

ILK, an important serine/threonine protein phosphatase, serves a key role in the regulation of signal transduction and

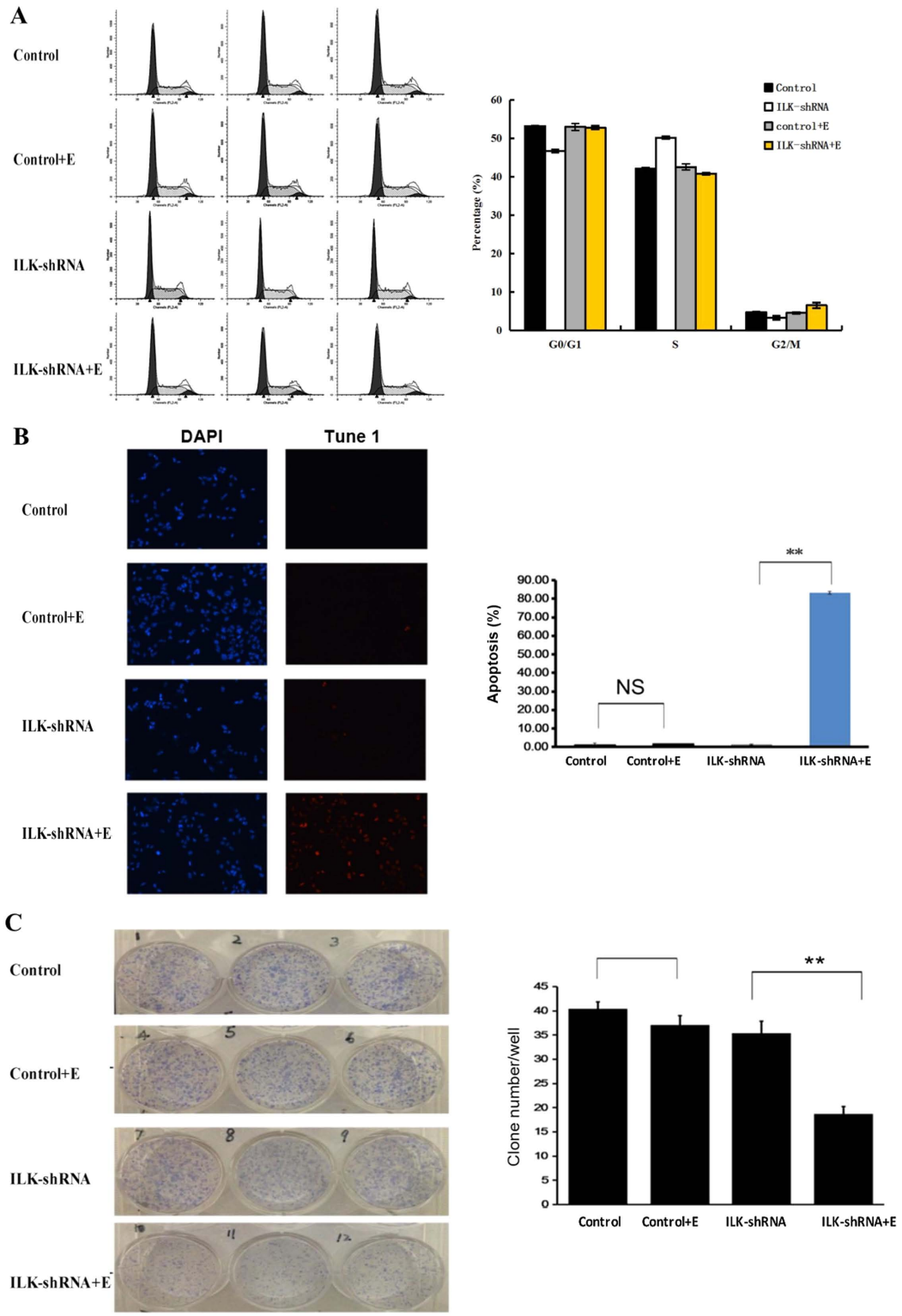

Figure 4. Effects of ILK on erlotinib resistance in lung squamous cell carcinoma cells. (A) ILK knockout caused cell cycle arrest at S phase, erlotinib caused cell cycle arrest at G_0/G_1 phase, and ILK knockout and erlotinib caused cell cycle arrest at the G_2/M phase. (B) The results of the TUNEL assay demonstrated that the apoptosis rate was higher in cells treated with erlotinib after ILK knockdown compared with those treated with erlotinib alone. (C) The ability of cell clone formation significantly decreased in the group treated with erlotinib after ILK knockdown compared with that in the group treated with erlotinib alone. **P<0.01. SqCC, squamous cell carcinoma; ILK, integrin-linked kinase; siRNA, small interfering RNA; NC, negative control; E, erlotinib.

remodeling of the tumor extracellular matrix (ECM) (25). High expression of ILK is associated with the occurrence and development of lung cancer, as well as with anti-cancer drug resistance, including resistance to EGFR-TKIs (26-31); thus, it was hypothesized that ILK may be a target for reversing erlotinib resistance. The results of the present study confirmed that the expression of ILK was remarkably higher in patients with lung SqCC compared with that in patients with adenocarcinoma with sensitizing EGFR mutations, suggesting that ILK may be a key marker of EGFR-TKI resistance in lung SqCC.

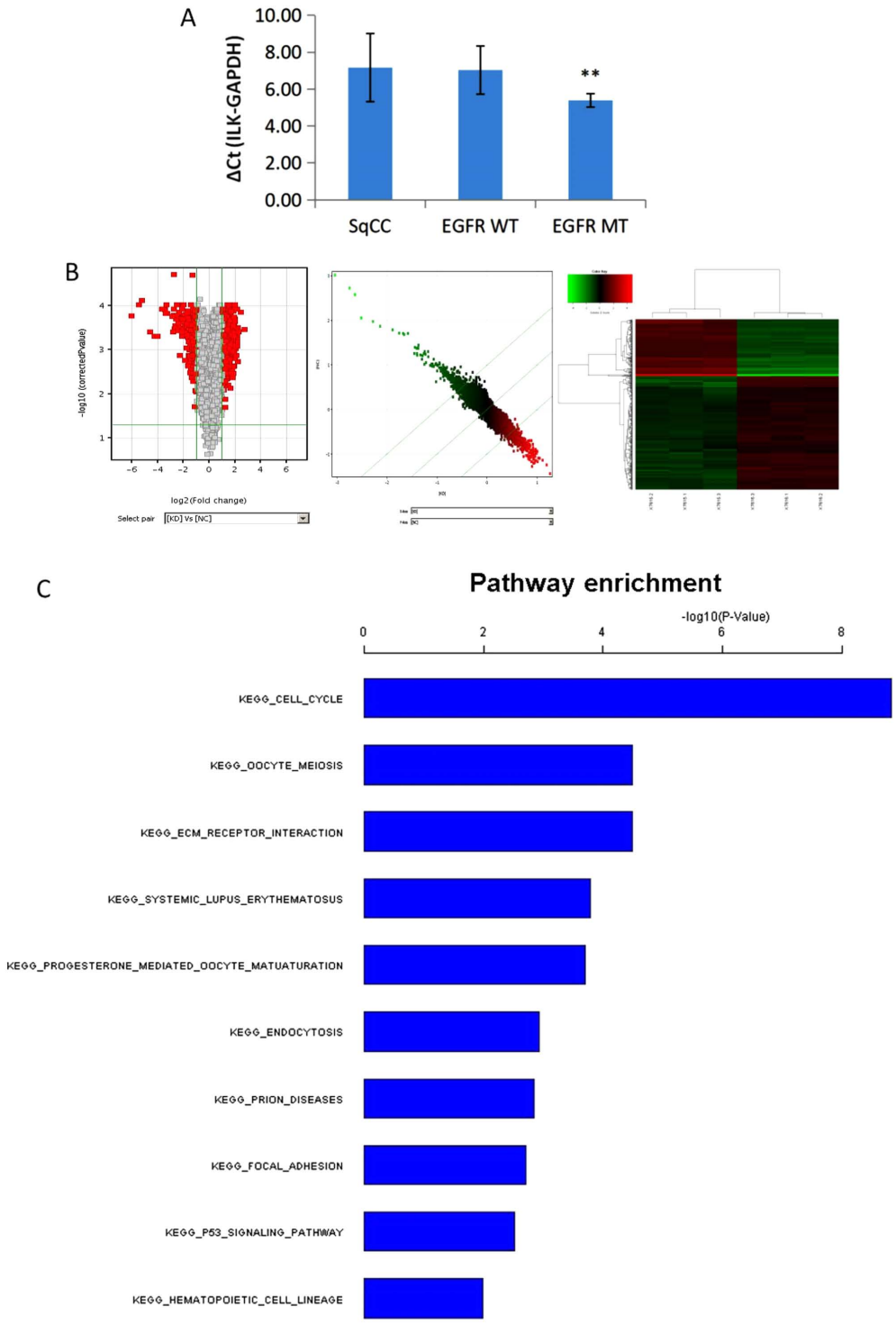

Figure 5. Expression of ILK and genome-wide transcriptional analysis of the key pathways of ILK. (A) The expression of ILK in patients with lung SqCC was significantly higher compared with that in patients with adenocarcinoma with EGFR mutation (**P<0.01). No significant differences were observed between patients with wild-type EGFR adenocarcinoma and SqCC. (B) A total of 484 differentially expressed transcripts (317 upregulated and 167 downregulated) in the KD group compared with the NC group, based on fold-change >2 and P<0.05 threshold, passed the filtering process and were used for the cluster analysis. In the volcano map, the x-axis shows the negative log of P-value calculated by t-test, and the y-axis shows the converted value after $\log_2$ transformation under the comparison of the KD and NC groups. Scatter plot and heatmap showed the overall distribution and concentration trend of two groups of data. (C) Functional analysis of the gene expression profiling using pathways analysis according to the KEGG and BioCarta Database revealed that the top three targets enriched by ILK knockdown were the 'cell cycle', 'ECM receptor interaction' and 'oocyte meiosis'. SqCC, squamous cell carcinoma; ILK, integrin-linked kinase; WT, wild-type; MT, mutated; KEGG, Kyoto Encyclopedia of Genes and Genomes; ECM, extracellular matrix KD, SK-MES-1 cells treated with erlotinib after ILK knockdown; NC, negative control.

To gain further insight into the mechanism of ILK in the resistance of lung SqCC to EGFR-TKIs, KEGG, GO and IPA were used to explore the associated signaling pathways and gene networks in the present study. The 'cell cycle', 'oocyte meiosis, 'ECM-receptor interaction', 'protein kinase activity' and 'DNA binding' were identified to be closely

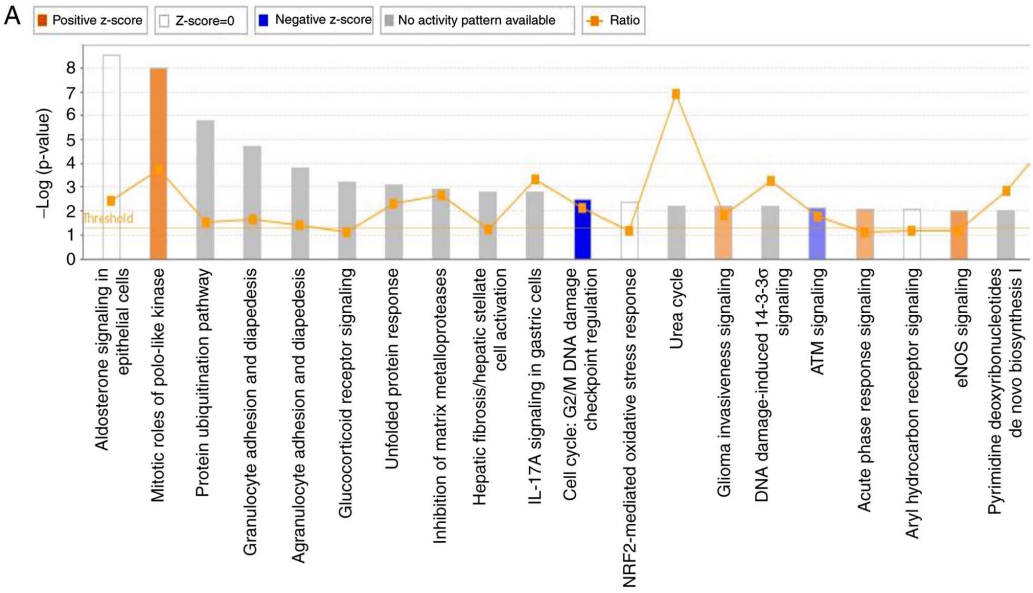

B

ID	Molecules in Network	Score	Focus Mol	Top Diseases and Functions
1	↓AGR2*, ↑ARHGEF28, ↑ASPM*, ↑AURKB, ↑B4GALNT1, ↑BUB1, ↑BUB1B, ↑CASC5, Cdc2, ↑CDC20*, ↑CENPA*, ↑CENPI, ↑CENPK, ↑CENPN, ↑CENPW, Cyclin B, ↑DSN1, ↓FAM46C*, ↓FOS*, ↑FOXM1, ↑KIF11, ↑KIF20A, Mpf, ↑NDC80, ↑NUF2, Plk, ↑PLK4, ↑SKA1*, ↑SKA3, ↑SPC24, ↑SPC25, ↑STIL*, ↑TAX1BP3, ↑TTK, ↑ZWINT*	46	31	Cell Cycle, Cellular Assembly and Organization, DNA Replication, Recombination, and Repair
2	Akt, ↓CCDC117, Collagen type VI, ↑CPE, ↓DDIT4, ↓DNAJA1*, ↓DNAJA4*, ↓DNAJB1*, ↓DNAJB4*, ↓DNAJC24, ↓ELOVL5, ↓FOXC1, Hdac, HSP, Hsp22/Hsp40/Hsp90, ↓HSPA6, ↓HSPA1A/HSPA1B*, ↓HSPA1L, ↓HSPA4L*, ↓HSPB8*, ↓HSPE1, ↓HSPH1*, ↑LPXN, ↑PBK, ↑PDE5A, ↑PHLDA1*, Pkg, Ppp2c, Ptk, ↑PTK7, ↑RNF207, ↑SEMA7A, SERCA, ↓STIP1*, ↑TACSTD2	40	26	Cellular Compromise, Cellular Function and Maintenance, Post-Translational Modification
3	↑ABCC3, ↓ARG2, arginase, ATPase, ↓BANP*, ↑BLM, ↑CIT, cyclooxygenase, ↑ERCC6L, Erm, ↑EXO1, F Actin, ↑FGFBP1, ↓JDP2, ↑KIF14, ↑KIF23*, ↑KIF2C*, ↑KIF4A, ↑KIFC1, ↑NCAPG, ↑NCAPH, Nos, ↑OLR1, P glycoprotein, PARP, Pkc(s), Plc beta, ↑PRC1*, ↑PRSS23*, ↑PTGFRN, ↑RACGAP1, ↓RGS2, ↑SHCBP1*, ↑TROAP*, ↓ZC3HAV1	39	25	Cell Cycle, Cellular Movement, Cellular Assembly and Organization
4	alcohol group acceptor phosphotransferase, Angiotensin II receptor type 1, ↑CDC23, ↑CDK1*, ↑CDKN3*, ↑CENPF*, Cpla2, ↑DGKQ, ↑DNER, ↑EHF*, ↑ESPL1, ↓HES1, ↑HJURP, ↑HMMR*, ↑HSPG2, Il8r, ↑KIF18A, ↑MELK, ↑MKI67*, MTORC2, ↑NEK2*, Neuropilin, Notch, ↑NRP1, ↑NT5E, ↓PGF, ↑PTTG1, Secretase gamma, ↑SERPINB2, ↑SGK1*, ↓SPRR2D*, ↑SSPN, trypsin, Vegf, ↑VEGFC	38	25	Cancer, Organismal Injury and Abnormalities, Cellular Movement
5	↑ARL4A, ↑BMP1, ↓BMP4, ↓BTG3, ↑CDCA5, Collagen type II, Collagen type III, Collagen type V, Ctbp, ↑DKK1, ↓DLX2, ERK, ↑FBN1, ↓HEY1, Igfbp, ↑IGFBP7, ↓ILK, ↑LAMB1, Laminin1, ↓LEFTY1, ↑LUM, ↓MSX1, ↑NEXN*, ↑PDCD1LG2, ↑RUNX2, ↑SCLT1, Smad1/5/8, Smad2/3, SMOOTH MUSCLE ACTIN, TCF, TMSB4, ↑TNC, ↑TPM1*, ↑UGCG, ↑VCAN*	34	23	Connective Tissue Developmen and Function, Organ Morphology, Organismal Development

Figure 6. Genome-wide transcriptional analysis of the key pathways of ILK in EGFR-TKI resistance of SK-MES-1 cell line. (A) IPA results identified that the 'cell cycle: G2/M DNA damage and checkpoint regulation' pathway (Z-score, -2) was significantly inhibited in the classic pathway analysis. (B) The IPA-based network analysis demonstrated that the ranked first network diagram in the present study mainly affected the cell cycle, cellular assembly organization, DNA replication, recombination and repair. ILK, integrin-linked kinase; IPA, ingenuity pathway analysis.

associated with the effects of ILK on EGFR-TKI resistance. As the cell cycle (32,33), ECM-receptor interaction (34,35) and mitosis (36) have been identified to be activated in cancer drug resistance, ILK may serve a crucial role in the EGFR-TKI resistance of lung SqCC via these pathways. GO analysis results also demonstrated that 'mitotic cell cycle' and 'mitosis' were important signaling pathways involved in EGFR-TKI resistance in ILK-knockout cells. IPA further confirmed that 'cell cycle: G_2/M DNA damage checkpoint regulation' was the most key signaling pathway regulated by ILK knockout in the EGFR-TKI resistance of lung SqCC. In conclusion, ILK may improve our understanding of lung SqCC and may be a future therapeutic target.

Acknowledgements

Not applicable.

Funding

This work was supported by the National Natural Science Foundation of China (grant no. 81207106), the Science and Technology Commission of Shanghai Municipality (grant nos. 17401932400 and 19401930800) and Shanghai Pulmonary Hospital (grant no. fkgg1807).

Availability of data and materials

The datasets used and/or analyzed during the present study are available from the corresponding author on reasonable request.

Authors' contributions

LJ conceived and designed the study. ZD and JY acquired, analyzed and interpreted the data and drafted the manuscript. ML analyzed the data and revised the manuscript critically for important intellectual content. All authors read and approved the final manuscript.

Ethics approval and consent to participate

The study was approved by The Ethics Committee of Shanghai Pulmonary Hospital (Shanghai, China). Signed informed consents were obtained from the patients and/or guardians.

Patient consent for publication

Not applicable.

Competing interests

The authors declare that they have no competing interests.

References

1. Wahbah M, Boroumand N, Castro C, El-Zeky F and Eltorky M: Changing trends in the distribution of the histologic types of lung cancer: A review of 4439 cases. Ann Diagn Pathol 11: 89-96, 2007.
2. Camidge DR, Doebele RC and Kerr KM: Comparing and contrasting predictive biomarkers for immunotherapy and targeted therapy of NSCLC. Nat Rev Clin Oncol 16: 341-355, 2019.
3. Sands JM, Nguyen T, Shivdasani P, Sacher AG, Cheng ML, Alden RS, Jänne PA, Kuo FC, Oxnard GR and Sholl LM: Next-generation sequencing informs diagnosis and identifies unexpected therapeutic targets in lung squamous cell carcinomas. Lung Cancer 140: 35-41, 2020.
4. National Comprehensive Cancer Network (NCCN). Clinical Practice Guidelines in Oncology. Plymouth, PA, 2018.
5. Mok TSK, Wu YL, Kudaba I, Kowalski DM, Cho BC, Turna HZ, Castro G Jr, Srimuninnimit V, Laktionov KK, Bondarenko I, *et al*: Pembrolizumab versus chemotherapy for previously untreated, PD-L1-expressing, locally advanced or metastatic non-small-cell lung cancer (KEYNOTE-042): A randomised, open-label, controlled, phase 3 trial. Lancet 393: 1819-1830, 2019.
6. Hochmair MJ, Morabito A, Hao D, Yang CT, Soo RA, Yang JC, Gucalp R, Halmos B, Wang L, Märten A and Cufer T: Sequential afatinib and osimertinib in patients with EGFR mutation-positive non-small-cell lung cancer: Updated analysis of the observational GioTag study. Future Oncol 15: 2905-2914, 2019
7. Brahmer J, Reckamp KL, Baas P, Crinò L, Eberhardt WE, Poddubskaya E, Antonia S, Pluzanski A, Vokes EE, Holgado E, *et al*: Nivolumab versus Docetaxel in advanced squamous-cell non-small-cell lung cancer. N Engl J Med 373: 123-135, 2015.
8. Herbst RS, Baas P, Kim DW, Felip E, Pérez-Gracia JL, Han JY, Molina J, Kim JH, Arvis CD, Ahn MJ, *et al*: Pembrolizumab versus docetaxel for previously treated, PD-L1-positive, advanced non-small-cell lung cancer (KEYNOTE-010): A randomised controlled trial. Lancet 387: 1540-1550, 2016.
9. Solassol I, Pinguet F and Quantin X: FDA- and EMA-approved tyrosine kinase inhibitors in advanced *EGFR*-mutated non-small cell lung cancer: Safety, tolerability, plasma concentration monitoring, and management. Biomolecules 9: 668, 2019.
10. Hirsch FR, Varella-Garcia M, Bunn PA Jr, Di Maria MV, Veve R, Bremmes RM, Barón AE, Zeng C and Franklin WA: Epidermal growth factor receptor in non-small-cell lung carcinomas: Correlation between gene copy number and protein expression and impact on prognosis. J Clin Oncol 21: 3798-3807, 2003.
11. Cancer Genome Atlas Research Network: Comprehensive genomic characterization of squamous cell lung cancers. Nature 489: 519-525, 2012.
12. Wang Z, Shen Z, Li Z, Duan J, Fu S, Liu Z, Bai H, Zhang Z, Zhao J, Wang X and Wang J: Activation of the BMP-BMPR pathway conferred resistance to EGFR-TKIs inlung squamous cell carcinoma patients with EGFR mutations. Proc Natl Acad Sci USA 112: 9990-9995, 2015.
13. Hata A, Katakami N, Yoshioka H, Kunimasa K, Fujita S, Kaji R, Notohara K, Imai Y, Tachikawa R, Tomii K, *et al*: How sensitive are epidermal growth factor receptor-tyrosine kinase inhibitors for squamous cell carcinoma of the lung harboring EGFR gene-sensitive mutations? J Thorac Oncol 8: 89-95, 2013.
14. Shukuya T, Takahashi T, Kaira R, Ono A, Nakamura Y, Tsuya A, Kenmotsu H, Naito T, Kaira K, Murakami H, *et al*: Efficacy of gefitinib for non-adenocarcinoma non-small-cell lung cancer patients harboring epidermal growth factor receptor mutations: A pooled analysis of published reports. Cancer Sci 102: 1032-1037, 2011.
15. Filipits M: New developments in the treatment of squamous cell lung cancer. Curr Opin Oncol 26: 152-158, 2014.
16. Schwaederle M, Elkin SK, Tomson BN, Carter JL and Kurzrock R: Squamousness: Next-generation sequencing reveals shared molecular features across squamous tumor types. Cell Cycle 14: 2355-2361, 2015.
17. Goss GD and Spaans JN: Epidermal growth factor receptor inhibition in the management of squamous cell carcinoma of the lung. Oncologist 21: 205-213, 2016.
18. Memon AA, Zhang H, Gu Y, Luo Q, Shi J, Deng Z, Ma J and Ma W: EGFR with TKI-sensitive mutations in exon 19 is highly expressed and frequently detected in Chinese patients with lung squamous carcinoma. Onco Targets Ther 10: 4607-4613, 2017.
19. Livak KJ and Schmittgen TD: Analysis of relative gene expression data using real-time quantitative PCR and the 2(-Delta Delta C(T)) method. Methods 25: 402-408, 2001.
20. Ray P, Raghunathan K, Ahsan A, Allam US, Shukla S, Basrur V, Veatch S, Lawrence TS, Nyati MK and Ray D: Ubiquitin ligase SMURF2 enhances epidermal growth factor receptor stability and tyrosine-kinase inhibitor resistance. J Biol Chem 295: 12661-12673, 2020.
21. Lei T, Zhang L, Song Y, Wang B, Shen Y, Zhang N and Yang M: *miR-1262* Transcriptionally modulated by an enhancer genetic variant improves efficiency of epidermal growth factor receptor-tyrosine kinase inhibitors in advanced lung adenocarcinoma. DNA Cell Biol 39: 1111-1118, 2020.
22. Nilsson MB, Sun H, Robichaux J, Pfeifer M, McDermott U, Travers J, Diao L, Xi Y, Tong P, Shen L, *et al*: A YAP/FOXM1 axis mediates EMT-associated EGFR inhibitor resistance and increased expression of spindle assembly checkpoint components. Sci Transl Med 12: eaaz4589, 2020.
23. Rong X, Liang Y, Han Q, Zhao Y, Jiang G, Zhang X, Lin X, Liu Y, Zhang Y, Han X, *et al*: Molecular mechanisms of tyrosine kinase inhibitor resistance induced by membranous/cytoplasmic/nuclear translocation of epidermal growth factor receptor. J Thorac Oncol 14: 1766-1783, 2019.
24. Pinheiro FD, Teixeira AF, de Brito BB, da Silva FAF, Santos MLC and de Melo FF: Immunotherapy-new perspective in lung cancer. World J Clin Oncol 11: 250-259, 2020.
25. Assi K, Bergstrom K, Vallance B, Owen D and Salh B: Requirement of epithelial integrin-linked kinase for facilitation of Citrobacter rodentium-induced colitis. BMC Gastroenterol 13: 137, 2013.
26. Chen D, Zhang Y, Zhang X, Li J, Han B, Liu S, Wang L, Ling Y, Mao S and Wang X: Overexpression of integrin-linked kinase correlates with malignant phenotype in non-small cell lung cancer and promotes lung cancer cell invasion and migration via regulating epithelial-mesenchymal transition (EMT)-related genes. Acta Histochem 115: 128-136, 2013.
27. Espinoza I and Miele L: Deadly crosstalk: Notch signaling at the intersection of EMT and cancer stem cells. Cancer Lett 341: 41-45, 2013.
28. Yu J, Shi R, Zhang D, Wang E and Qiu X: Expression of integrin-linked kinase in lung squamous cell carcinoma and adenocarcinoma: Correlation with E-cadherin expression, tumor microvessel density and clinical outcome. Virchows Arch 458: 99-107, 2011.
29. Posch F, Setinek U, Flores RM, Bernhard D, Hannigan GE, Mueller MR and Watzka SB: Serum integrin-linked kinase (sILK) concentration and survival in non-small cell lung cancer: A pilot study. Clin Transl Oncol 16: 455-462, 2014.
30. Jia Z: Role of integrin-linked kinase in drug resistance of lung cancer. Onco Targets Ther 8: 1561-1565, 2015.
31. Augustin A, Lamerz J, Meistermann H, Golling S, Scheiblich S, Hermann JC, Duchateau-Nguyen G, Tzouros M, Avila DW, Langen H, *et al*: Quantitative chemical proteomics profiling differentiates erlotinib from gefitinib in EGFR wild-type non-small cell lung carcinoma cell lines. Mol Cancer Ther 12: 520-529, 2013.
32. Liu M, Xu S, Wang Y, Li Y, Li Y, Zhang H, Liu H and Chen J: PD 0332991, a selective cyclin D kinase 4/6 inhibitor, sensitizes lung cancer cells to treatment with epidermal growth factor receptor tyrosine kinase inhibitors. Oncotarget 7: 84951-84964, 2016.
33. Dermawan JK, Gurova K, Pink J, Dowlati A, De S, Narla G, Sharma N and Stark GR: Quinacrine overcomes resistance to erlotinib by inhibiting FACT, NF-κB, and cell-cycle progression in non-small cell lung cancer. Mol Cancer Ther 13: 2203-2214, 2014.
34. Kaylan KB, Gentile SD, Milling LE, Bhinge KN, Kosari F and Underhill GH: Mapping lung tumor cell drug responses as a function of matrix context and genotype using cell microarrays. Integr Biol (Camb) 8: 1221-1231, 2016.
35. Wang J, Wang B, Chu H and Yao Y: Intrinsic resistance to EGFR tyrosine kinase inhibitors in advanced non-small-cell lung cancer with activating EGFR mutations. Onco Targets Ther 9: 3711-3726, 2016.
36. Salmela AL and Kallio MJ: Mitosis as an anti-cancer drug target. Chromosoma 122: 431-449, 2013.